




¹⁴C MICROSAMPLE ANALYSIS WITH ECHOMICADAS FACILITIES: CURRENT STATE OF PLAY

François Thil^{1*}  • Nadine Tisnérat-Laborde¹ • Christine Hatté^{1,2}  • Elias Kader¹ • Claude Noury¹ • Martine Paterne¹ • Brian Phouybanhdyt¹ • Lukas Wacker³ 

¹Laboratoire des Sciences du Climat et de l'Environnement, IPSL/LSCE, CEA CNRS UVSQ, Université Paris-Saclay, F-91191, Gif Sur Yvette, France

²Division of Geochronology and Environmental Sciences, Institute of Physics, Silesian University of Technology, 44-100 Gliwice, Poland

³Ion Beam Physics, Department of Physics, ETH Zürich, HPK H29, Otto-Stern-Weg 5, 8093 Zürich, Switzerland

ABSTRACT. In 2015, a new accelerator mass spectrometry facility (AMS), the ECHoMICADAS (Environnement, Climat, Homme, Mini Carbon Dating System), was installed in the Laboratoire des Sciences du Climat et de l'Environnement (LSCE). Equipped with a hybrid source, it allows the analysis of solid or gas samples for ¹⁴C measurement. Here, we summarize the equipment surrounding the Gas Interface System (GIS), namely the elemental analyzer (EA), the carbonate handling system (CHS2) and the ampoule cracker. We describe our model of sample contamination, taking into account the cross and the constant contaminations, and then describe how these contaminations were handled in the data processing. Both contaminant corrections are applied before the phases of blank subtraction and standard normalization, making it possible to use the standard, blank and sample ratios without contaminant during these phases. We finally present our results on normalization standards (N=118), blanks (N=125) and reference materials (N=117) for different measurement protocols and for sample masses between 3 and 300 µgC.

KEYWORDS: ¹⁴C dating, carbonate handling system, contaminant correction, elemental analyzer, gas interface system.

INTRODUCTION

Since 2015, the radiocarbon dating facility at the Laboratoire des Sciences du Climat et de l'Environnement (LSCE) has operated an accelerator mass spectrometer (AMS), the ECHoMICADAS (Environnement, Climat, Homme Mini Carbon Dating System). It is a 200kV AMS and results from an updated version of the MICADAS series (Synal et al. 2007) designed by ETH Zürich that comprises three identical instruments: ECHoMICADAS (Tisnérat-Laborde et al. 2015), BRIS-MICADAS (Knowles et al. 2019) and a third one operated by ETH Zürich. The three of them are characterized by a helium stripper and two permanent magnets for low and high energy.

Equipped with a versatile source, ECHoMICADAS is able to run either 40 graphite targets on a magazine (sample size from 0.3 to 1 mgC) or CO₂ gas samples (from 3 to 300 µgC) injected into the source through a Gas Interface System (GIS, Ionplus society) (Ruff et al. 2007). The GIS is connected either to an ampoule cracker system, an elemental analyzer (EA) or a carbonate handling system (CHS2). The technical possibility of measuring small samples is an advantage but is associated with a relatively greater effect of contamination on the ¹⁴C activities than for large mass samples. For solid measurement, it is possible to run the sequence with mass-homogenous samples (often 1 mgC), and the contaminant is negligible compared to the sample material. The contaminant correction is indirectly considered when normalizing with standards and blanks with the same mass as the samples. For smaller samples, until now, this correction was done after data reduction, from the F¹⁴C values, but the way the data are processed is not clearly addressed in publications. The purpose of this study is to reexamine traditional calculations in accelerator mass spectrometry by integrating the contaminant

*Corresponding author. Email: francois.thil@lsce.ipsl.fr

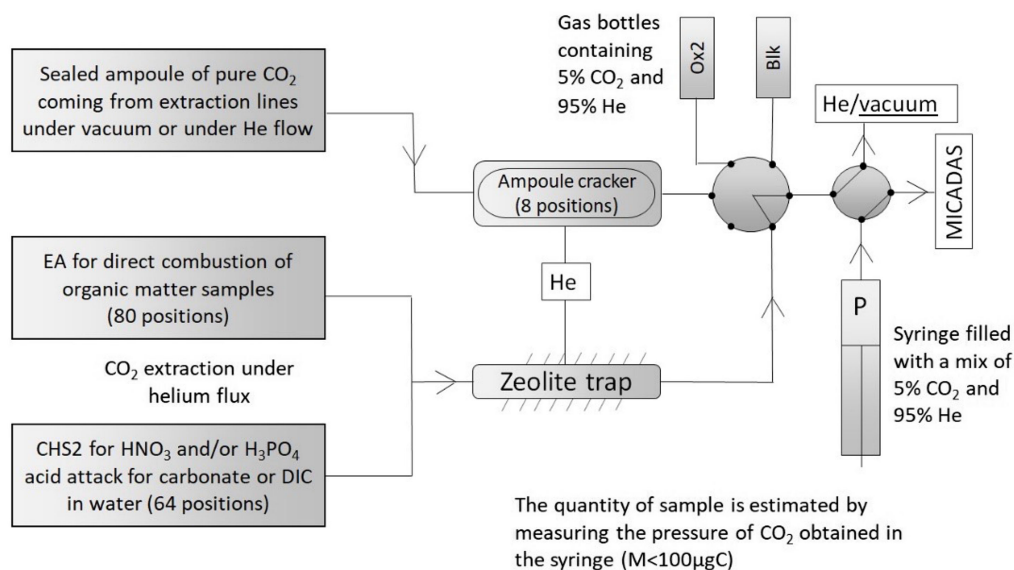


Figure 1 ECHoMICADAS GIS equipment. Three introduction possibilities: Elemental analyzer (EA), Carbonate Handling System (CHS2), and ampoule cracker system. In this configuration, the syringe is connected to the AMS while the CO₂ from the EA or the CHS2 is fixed on the cold zeolite trap (22°C). Once the syringe is empty, it is connected to the zeolite trap; the trap, which is heated to 450°C, releases the CO₂ in the syringe.

correction into the data processing. We propose here to apply this contaminant correction before blank subtraction and normalization. This enables the whole sequence to be normalized, whatever the standards, blanks and sample sizes. Results will be given on different blanks, normalization and reference standards.

METHODS

AMS ECHoMICADAS and Its Peripheral Instruments

The ECHoMICADAS AMS is equipped with a hybrid source that measures solid or gas samples (Ruff et al. 2007). The GIS software (version 4.6.1) is used to operate all the other peripheral instruments and to coordinate the MICADAS software to start the analysis at the right time. As shown in Figure 1, the GIS offers 3 possibilities to introduce the CO₂ gas samples: (1) pure CO₂, obtained off-line, is directly delivered to the syringe by the ampoule cracker system (Ruff et al. 2007), or the CO₂ is transferred on-line from (2) an Elemental Analyzer (Ruff et al. 2010a) or (3) a Carbonate Handling System (Wacker et al. 2013) in a helium flow (purity 5.7) to a zeolite trap (Zeolite 13X, supplied by Supelco). By heating this trap, the pure CO₂ is released and quantified in the syringe by pressure measurement. In all three cases, in the syringe, the pure CO₂ is mixed with 95% He (purity 5.2) before being injected at constant flow into the MICADAS source. Carbon current is maximized with a CO₂/He ratio of 5%/95%. However, for very small samples (<6 μgC), the CO₂ is often over-diluted to less than 5%. In this case the operator has to increase the He+CO₂ pressure manually during the measurement by reducing the syringe volume, in order to keep the carbon current as high and as stable as possible. The ampoule cracker and the elemental analyzer systems were installed at LSCE in 2016 and the CHS2 in 2021.

Elemental Analyzer/GIS

The Elemental Analyzer (Vario ISOTOPE Select, Elementar) is used to analyze sequentially the CO₂ released from solid organic/bulk sample combustion (up to 80 positions). The solid sample is wrapped in a tin capsule (at LSCE, 5 × 9 mm or 3.3 × 5 mm capsules, Säntis Analytical, without pretreatment). The size of the capsule depends on the sample size, the carbon content and the sample type. The capsule is combusted in the EA where N and C fractions are sequentially quantified. The C fraction is carried to the GIS by helium flux. Analyses with the EA are prone to contamination from (1) carbons that could not be removed, (2) carbon that might be introduced during the chemistry step, (3) contamination from the capsule (Ruff et al. 2010a), and in particular from the organo-metallic interactions that can occur on its surface, and (4) residual carbon contaminant coming from the previous sample which might have accumulated in the line, especially on the EA carbon trap, on the GIS zeolite trap, and in the capillaries.

Carbonate Handling System/GIS

The CHS2 (Ionplus company) is an autosampler (64 positions) with a heating block. The equipment is used to automate two types of operation: (1) the acidification of the samples via a 5 mL syringe (the reaction is thermoregulated at 80°C) and (2) the CO₂ gas transfer under Helium flux via a double syringe. The carbonate sample is placed in a 4.5 mL vial with a septum cap. To clean the sample surface, leaching can be performed by adding 100 µL of 0.01N HNO₃ for 15 min. Then, the vial is flushed by Helium flux (60 mL/min during 3 min) and next the carbonate is completely dissolved by adding 500 µL of H₃PO₄. After at least 30 min, the CO₂ produced is carried through a water trap (Sicapent, Merck) and then transferred by helium flux (60 mL/min, during 1 min) onto the zeolite trap. The sequence is automated via the GIS software where for each sample, a specific protocol can be planned (type of acid, acid volume, acidification duration, sampling time via the double syringe).

Ampoule Cracker/GIS

The Ampoule cracker system is particularly suitable for short series of samples (the cracker is limited to 8 sample positions). It was first described in Ruff et al. (2007), and characterized in greater detail in Ruff et al. (2010b) and Fahrni et al. (2010). Ampoules contain pure CO₂, extracted from carbonate or organic matter samples and sealed, using LSCE preparation lines, as described in Hatté et al. 2023. One of these lines, the “BCA” (in French, Banc Carbonate Automatisé: Automated Carbonate Bench) is dedicated to CO₂ extraction from carbonate samples. The carbonate is previously cleaned with HNO₃ 0.01N solution and then hydrolyzed on the BCA line by adding H₃PO₄ solution (Tisnérat-Laborde et al. 2001). The pure CO₂ is collected in a cold trap and sealed in ampoules.

Standard Materials

The data reported in the Results section (Figure 3 and Table 1) were all measured in 2021 and 2022. We analyzed 320 organic standards, in the range from 3 to 300 µgC through the EA-GIS interface and carbonate standards through the CHS2-GIS (n=71, 3 to 300 µgC) or ampoule cracker-GIS system (n=49, 3 to 300 µgC). We ran the most common standards of organic matter: phthalic acid (noted PHA, F¹⁴C = 0), oxalic acid II NIST SRM 4990C (noted Oxa2, F¹⁴C = 1.3406), and the IAEA oxalic acid reference materials IAEA-C7 (F¹⁴C = 0.4951) and IAEA-C8 (F¹⁴C = 0.1503). For carbonates, we used the IAEA-C1 marble as a blank (F¹⁴C = 0) and IAEA-C2 travertine as a reference material (F¹⁴C = 0.4114). As there is no ¹⁴C/¹²C active carbonate standard, we used an in-house standard with an active ¹⁴C/¹²C ratio (F¹⁴C = 1.20) to better estimate the constant contamination. This standard is a mollusk shell

Patella Vulgata collected in 1970. Concerning carbonate standards and samples, leaching was previously done (100 μL HNO_3 0.01N, added in the vial of the CHS2 or in the reactor of the BCA line). Concerning the organic matter standards, no pretreatment was done on the sample or on the EA capsule.

In the Results section, we also report in Figure 4 all IAEA-C1 and IAEA-C2 data measured from 2016 to 2022 via the ampoule cracker system to demonstrate the absence of contamination during storage in the tube.

Sequence Construction and Acquisition Parameters

Samples are always included in an acquisition sequence which may last between half a day and 3 days of measurement. For long sequences, the 40-position magazine is replenished every 8 hours. The sequence contains Oxa2 standards for normalization and blanks (generally only larger masses are considered: $m > 75 \mu\text{gC}$), chemical standards and chemical blanks, and smaller standards and blanks (when possible, with masses between 3 and 50 μgC in order to evaluate or partially re-evaluate the constant contaminant, as often as possible). Analyses are ordered from the oldest to the youngest to minimize cross-contamination (as proposed by Wacker et al. 2013). For each cathode, the total measurement time is close to 15 min for masses greater than 40 μgC and is directly proportional to the carbon mass for lower masses. This measurement time is subdivided into smaller integration points with a sampling period of 10s/5s (for masses higher/lower than 10 μgC respectively). The high energy ^{12}C current is between 5 to 9 μA . Measurement points with a current below 3 μA or with a noisy $^{13}\text{C}/^{12}\text{C}$ value are manually removed from the raw data.

DATA PROCESSING

To process the data for large samples ($>300 \mu\text{gC}$) the BATS software (Wacker et al. 2010) is generally used at LSCE. For smaller samples ($<300 \mu\text{gC}$), the following raw data are exported from the BATS software to an Excel file: high energy currents ^{12}C , ^{13}C , $^{13}\text{Cmol}$ (^{13}C coming from the residual ^{13}CH molecules), ^{14}C counting, and the total integration time T . The sample mass is evaluated by the GIS software. These data are then processed in an Excel file to take into account the constant and cross contaminations which are described below.

Contamination Model

The contamination model is described in Figure 2a and is derived from Ruff et al. (2010a) and Salazar et al. (2015). It accounts for the constant contamination characterized by a constant carbon mass m_c , and a constant $^{14}\text{C}/^{12}\text{C}$ ratio r_c , as well as for the cross contamination proportional (factor ϕ) to the previous sample's carbon mass (m_0) with a known $^{14}\text{C}/^{12}\text{C}$ ratio (r_0). This model incorporates all the contamination originally contained in the samples and not extracted during the chemistry step as well as the carbon that might have been introduced during the handling process, from the chemistry to the CO_2 extraction and the measurement. We can reasonably use this model for masses greater than 10 μgC . For smaller masses, this model may no longer be accurate, because other parameters have to be considered such as (1) the surface contamination (e.g. related to the surface and therefore to the sample grain size), (2) the uncertainty on the GIS mass evaluation, or (3) the impact of low ^{12}C current sometimes due to an incorrect CO_2/He proportion, which degrades the blank values. The contamination parameters m_c , r_c are calculated as suggested in Hwang and Druffel (2005) by analyzing two different sample ratios (Oxa2 and PHA for example) several times with a large mass range

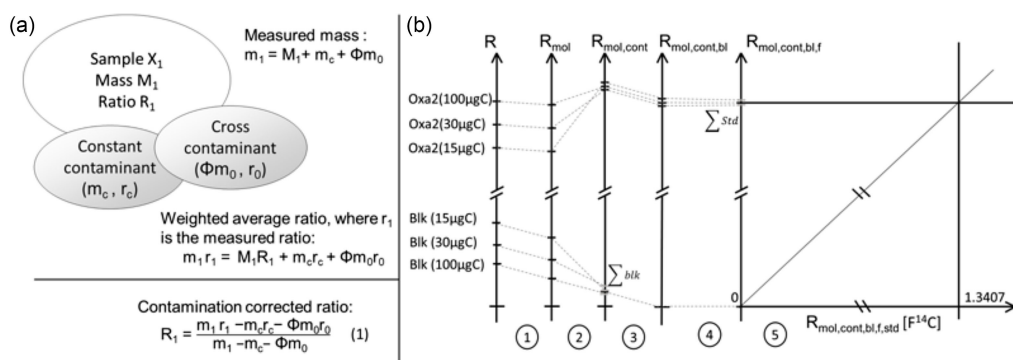


Figure 2 (a) Constant and cross contamination model; (b) Impact of the data reduction on two different ¹⁴C/¹²C ratios: Oxa2 and blank. Steps 1, 3, 4 and 5 are the same calculation steps as the ones applied in BATS software and are described in Wacker et al. (2010). Step 2 is added to take into account the mass of the sample. **Step 1:** molecular current ¹³CH correction. **Step 2:** contaminant correction based on the formula (1) described in Figure 2a. **Step 3:** blank correction **Step 4:** mass fractionation correction. **Step 5:** ratio normalization

(from 3 to 100 µgC). Their associated uncertainties σ_{r_c} , σ_{m_c} are evaluated by a Bayesian approach as suggested in Sun et al. (2020). The cross-contamination parameter Φ and its associated uncertainty σ_Φ represent a fraction of the previous measured sample and are determined by following the protocol given in Salazar et al. (2015) by intercalating fossil and modern samples.

Data Acquisition and Reduction

Data Reduction

In the following formulas, we have used the notation given in Wacker et al. (2010), where the subscripts *mol*, *cont*, *bl*, *f* and *std* refer respectively to the molecular correction (¹³Cmol), the contaminant correction, the blank subtraction, the fractionation correction and the standard normalization. Each calculation step is described below.

Step 1: In the first calculation step, the measured ¹⁴C/¹²C ratio is corrected for broken up molecules ¹³CH and this correction is proportional to the ¹³C_{mol} current and a factor k_{mol} , which is the same as in equation (3) of Wacker et al. (2010) and leads to $R(X)_{mol}$. This parameter is linked to the stripper potential of the AMS and its capability to totally break the molecule (for MICADAS, $k_{mol} = 150$)

$$R(X)_{mol} = \frac{^{14}\text{C} - k_{mol} * ^{13}\text{C}_{mol}}{^{12}\text{C}}$$

Step 2: This data reduction step is based on equation 1 in Figure 2a. In this step the ratio $R(X)_{mol,cont}$ is corrected for the constant and cross contaminant with the following formula:

$$R(X)_{mol,cont} = \frac{m_1 * R(X)_{mol} - m_c * r_c - \Phi * m_0 * R(X_0)_{mol}}{m_1 - m_c - \Phi * m_0}$$

The parameters m_1 and m_0 are the GIS measured mass of respectively the sample X and the previous sample X₀ in the measurement sequence; m_c , r_c are the parameters characterizing the constant contaminant (r_c is used in the formulas of this paper with the unit ¹⁴C /¹²C but is

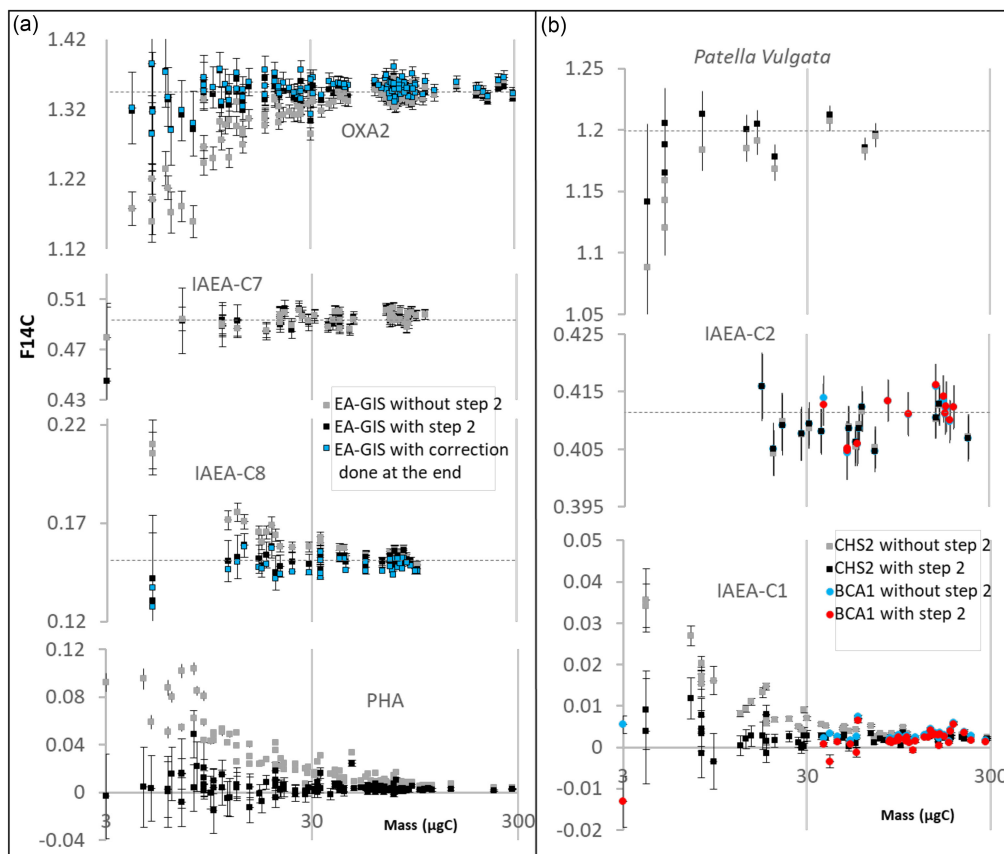


Figure 3 Standard and blank $F^{14}C$ values versus carbon mass, between 3 and 300 μgC (log scale). Only LSCE 2021 and 2022 measurements with high energy ^{12}C current higher than 3 μA are reported. Figure 3a—Organic matter standards and blanks measured on EA-GIS without step 2 (black squares), with step 2 (gray squares) and with the constant contaminant correction step done at the end (blue squares), Figure 3b—Carbonate standards (IAEA-C1 and IAEA-C2) and in-house standard (*Patella Vulgata*) measured on the CHS2-GIS (black and gray squares for ratio without or with step 2 correction) and measured via ampoule cracker-GIS (blue and red circles for ratios without or with step 2 correction).

recalculated in $F^{14}C$ units in the Results section); Φ is the cross contamination factor; $R(X)_{mol}$, $R(X_0)_{mol}$ are the molecular-interference-corrected ratios of respectively the sample itself and the previous sample.

Step 3: For this step, we first calculate the weighted mean of the blank. The weight factor p_i is the multiplication of the measurement time T_i by the $^{12}C_i$ current.

$$p_i = ^{12}C_i * T_i$$

$$\langle R(bl)_{mol,cont} \rangle = \frac{1}{\sum_i p_i} * \sum_i (p_i * R(bl_i)_{mol,cont})$$

Table 1 F¹⁴C values for the international standards oxalic acid II, IAEA-C2, IAEA-C7, IAEA-C8 and IAEA-C1 and phthalic acid (PHA) blanks. Blank values are reported without contaminant correction and blank subtraction. Three different means were calculated for masses higher than 100 µgC, medium masses between 35 and 100 µgC and masses lower than 35 µgC. The number of measurements N is given in brackets.

Intro-duction mode	Contaminant parameters	Sample type	F ¹⁴ C expected value	Mean F ¹⁴ C for m > 100 µgC	Standard deviation 1σ	F ¹⁴ C for medium mass	Standard deviation 1σ	Mean F ¹⁴ C for m < 35 µgC	Standard deviation 1σ
EA-GIS	$\Phi = 0.004 \pm 0.002$	Oxa2	1.3407	1.3421	0.0068 (12)	1.3408	0.0123 (57)	1.3399	0.0206 (49)
	$r_c \sim 0.6 \pm 0.12$	IAEA-C7	0.4951	0.4977	0.0039 (1)	0.4950	0.0046 (27)	0.4905	0.0137 (15)
	$m_c \sim 1.10 \pm 0.13 \mu\text{gC}$	IAEA-C8 PHA	0.1503 0.0000	no value 0.0050	no value 0.0012 (11)	0.1512 0.0099	0.0027 (21) 0.0045 (58)	0.1493 0.0415	0.0067 (17) 0.0250 (56)
CHS2-GIS	$\Phi = 0.004 \pm 0.002$	IAEA-C2	0.4114	0.4109	0.0030 (4)	0.4084	0.0034 (8)	0.4094	0.0040 (5)
	$r_c \sim 0.43 \pm 0.06$	IAEA-C1	0.0000	0.0033	0.0013 (9)	0.0040	0.0012 (13)	0.0133	0.0091 (22)
	$m_c \sim 0.31 \pm 0.13 \mu\text{gC}$								
Ampoule cracker GIS	$\Phi = 0$	IAEA-C2	0.4114	0.4120	0.0021 (6)	0.4081	0.0047 (3)	No value	No value
	$r_c \sim 0.6 \pm 0.12$	IAEA-C1	0.0000	0.0030	0.0011 (26)	0.0027	0.0015 (13)	0.0055	0.0021 (1)
	$m_c \sim 0.15 \pm 0.03 \mu\text{gC}$								

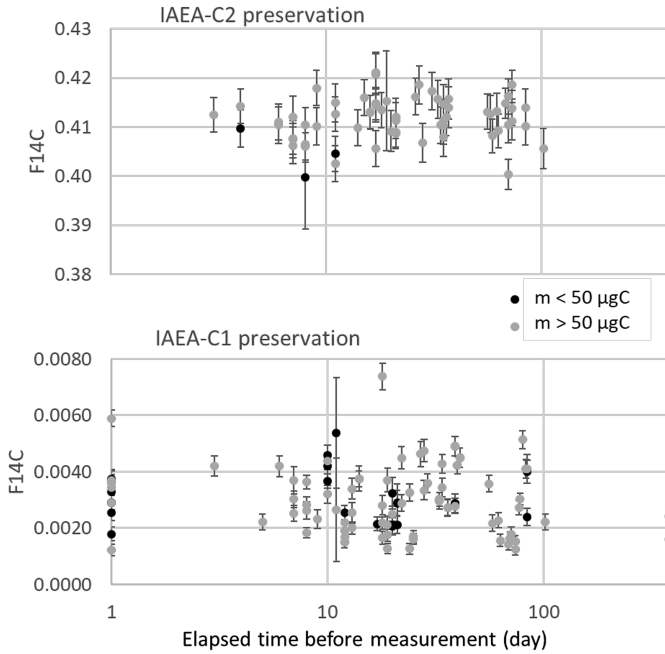


Figure 4 IAEA-C2 and IAEA-C1 $F^{14}C$ values versus elapsed time, between CO_2 sample tube sealing on the BCA line and cracker-GIS measurement on ECHoMICADAS. IAEA-C1 values are not corrected from blank and contaminant.

From this, the value corrected by the blank can be calculated:

$$R(X)_{mol,cont,bl} = R(X)_{mol,cont} - \langle R(bl)_{mol,cont} \rangle$$

For blank values, the $F^{14}C$ is generally given without applying step 2 and step 3.

Step 4: For this step, we first calculate the $^{13}C/^{12}C$ (noted $R_{13}(X)$) and the weighted mean of all the standard ratios (noted $R_{13}(Std)$) and we then calculate the $\delta^{13}C(X)$ as described in equation 6 of Wacker et al. (2010).

$$R_{13}(X) = \frac{^{13}C(X)}{^{12}C(X)}$$

$$\langle R_{13}(Std) \rangle = \frac{1}{\sum_i p_i} * \sum_i (p_i * R_{13}(std_i))$$

$$\delta^{13}C(X) = \left(\frac{R_{13}(X) * (1 + \delta^{13}C_{Std})}{\langle R_{13}(Std) \rangle} - 1 \right)$$

The fractionation correction is then applied to the $R(X)_{mol,cont,bl}$ as follows:

$$R(X)_{mol,cont,bl,f} = R(X)_{mol,cont,bl} * \left(\frac{0.975}{1 + \delta^{13}C(X)} \right)^2$$

Step 5: In order to normalize the sequence, the weighted mean value of the normalization standards is first calculated, based on the Oxa2 measured during the sequence:

$$\langle R(std)_{mol,cont,bl,f} \rangle = \frac{1}{\sum_i p_i} * \sum_i (p_i * R(std_i)_{mol,cont,bl,f})$$

The final $F^{14}C$ value can then be calculated:

$$R(X)_{mol,cont,bl,f,std} = \frac{R_{nom} * R(X)_{mol,cont,bl,f}}{\langle R(std)_{mol,cont,bl,f} \rangle}$$

Though not always made explicit in the literature (for example in Hua et al. 2004, Salazar et al. 2015 or Ruff et al. 2010a), the correction in step 2 is usually performed in other laboratories at the end, after step 5, as in these papers, the constant contaminant ratio is given in $\Delta^{14}C$, pMC or $F^{14}C$. At LSCE, this correction is done before blank subtraction and standard normalization. This idea was already suggested in Ruff et al. (2010b) but not fully applied or expressed. This procedure makes it possible to use “decontaminated” $^{14}C/^{12}C$ ratios which are more homogenous, whatever the blanks and the oxa2 masses are. As a result, the standard and blank masses which are used to normalize the sequence are not necessarily constrained to the sample masses.

Uncertainty Calculation

The complete uncertainty calculations are described step by step in Appendix A. The uncertainty formulas are obtained from the quadratic sum of the different partial derivatives of the previous formulas described from step 1 to 5. The final uncertainty takes into account the molecular correction uncertainty σ_{kmol} , the cross contaminant uncertainty σ_{Φ} , and the constant contaminant uncertainties σ_{r_c} and σ_{m_c} . For dispersion of the blanks, as in Wacker et al. (2010) or in Aerts-Bijma et al. (2021), we keep the possibility of increasing the blank variability measured during the sequence by increasing this variability to σ_{bl} , which takes into account the blank variability over a longer period: at LSCE this value is generally taken at 30% of the blank value. In the same way, we also keep the possibility of increasing the standard ratio variability by adding an external uncertainty σ_{ex} . For solid samples this value is around 0.15%. For GIS samples, this value has been increased to 0.5%. These 2 parameters σ_{bl} and σ_{ex} probably lead to an overestimation of the final uncertainty because they could be redundant with σ_{r_c} and σ_{m_c} .

For smaller masses, the final uncertainty will be degraded for several reasons: the first is linked to the low ^{14}C counting statistic, because the measurement integration time will be smaller; the second is linked to the constant contamination, especially if the sample ratio is far from the contamination ratio; the third is linked to the cross contamination, especially if the previously measured ratio is far from the sample ratio.

Critical Blank and Mass Values

In line with the recommendations of Stuiver and Polach (1977) to report ^{14}C age close to the background, we here adapt the conditions to report ^{14}C age close to the background for very small samples. To do so we compare the sample's $^{14}C/^{12}C$ ratio without blank and contaminant

correction ($R(X)_{mol,f,std}$) and a blank $^{14}C/^{12}C$ ratio with a similar mass measured in the sequence. If there is no available blank, we estimate the mass-equivalent blank ($R(Bl_equ)_{mol,f,std}$) with the following formulas, which calculate the equivalent blank according to the constant contaminant parameters (m_c , r_c) and to the sample mass m_1 :

$$R(Bl_equ)_{mol} = \langle R(bl)_{mol,cont} \rangle + \frac{m_c}{m_1} * (r_c - \langle R(bl)_{mol,cont} \rangle)$$

Then the step 4 correction is applied by calculating first $\delta^{13}C(Bl_equ) = \frac{1}{\sum_i p_i} * \sum_i (p_i * \delta^{13}C(bl_i))$ and step 5 correction is applied to obtain $R(Bl_equ)_{mol,f,std}$

From this calculation, we have the same 4 possibilities as in Stuiver and Polach (1977):

- If $R(X)_{mol,f,std} - 2\sigma(X)_{mol,f,std} < 0$ then age $> x$ where x is the radiocarbon age calculated for $R(X)_{mol,f,std} + 2\sigma(X)_{mol,f,std}$
- If $R(X)_{mol,f,std} - R(Bl_equ)_{mol,f,std} < 0$ then $R(X)_{mol,cont,bl,f,std} = 0$
- If $0 < R(X)_{mol,f,std} - R(Bl_equ)_{mol,f,std} < \sigma(X)_{mol,f,std}$ the $F^{14}C$ ratio of the sample is not distinguishable from the radiocarbon age of $R(Bl_equ)_{mol,f,std}$
- If $\sigma(X)_{mol,f,std} < R(X)_{mol,f,std} - R(Bl_equ)_{mol,f,std} < 2 * \sigma(X)_{mol,f,std}$ we can add the term “apparent” to the radiocarbon age calculated from $R(X)_{mol,cont,bl,f,std}$

RESULTS

Figure 3 shows the $F^{14}C$ results for GIS measurements with and without constant contamination correction (step 2 of the data processing) on organic and carbonate standards and blanks, analyzed in 2021 and 2022. Table 1 summarizes these data and gives the average $F^{14}C$ values for each standard (all within 1σ of the expected values) and blanks, for smaller, medium or high sample masses. The blank correction (step 3) is not applied to phthalic nor to IAEA-C1 values but is applied to all the other standards.

Organic Matter Results

The EA-GIS results on Figure 3a show that the contamination correction worked well for IAEA-C8, IAEA-C7 and Oxa2, as 99% of the results are within 2σ of the expected values. In Table 1 the average data are all within 1σ of the expected value. Concerning phthalic acid measurements, for masses $> 100 \mu gC$, ages are limited to 42.5 ± 1.9 ky BP (0.0050 ± 0.0012 $F^{14}C$) and are degraded to less than 25.6 ± 5.0 ky BP (0.0415 ± 0.0250) for smaller masses $< 35 \mu gC$.

The parameters m_c and r_c for EA-GIS were estimated from OXA2 and PHA measurements. A long-term temporal variation of these parameters (which does not appear in Figure 3a) has been observed since the beginning (in 2016). During this period, m_c has oscillated between 0.65 and 1.3 μgC , with a ratio r_c always close to 0.6 ($F^{14}C$). This r_c ratio is very close to IAEA-C7 values which explains why these values are almost unaffected by contaminant correction in Figure 3a. The constant contaminant parameters are comparable to the ones estimated by Salazar et al. (2015) or Bard et al. (2015) (respectively 1.4 μgC and 1.5 μgC with a $F^{14}C$ ratio around 0.7 and 0.5). We also noticed that when decreasing the capsule size (from 5×9 mm to

3.3 × 5 mm), the contaminant decreases to around 0.53 µgC. In Ruff et al. (2010a) for the smallest capsule, this contaminant was estimated at 0.3 µgC, with a ratio of 0.65. These differences may account for the direct procedure of estimating m_c with the EA and r_c from the analyses of 5 empty capsules at the same time, so only the contaminant of the capsule was taken into account. Concerning the cross-contamination effect, we estimated the parameter Φ at 0.004, but we observed that its occurrence was not systematic, which is why we associate a large uncertainty on this value ($\sigma_\Phi = 0.002$). In comparison, in Salazar et al. (2015), Φ was estimated at 0.002 ± 0.001 and in Ruff et al. (2010a), 0.004 (uncertainty was not specified).

Carbonate Results

Figure 3b reports the results from CHS2-GIS measurements (square symbols) and ampoule cracker measurements (circles). In both sample introduction modes, for IAEA-C2, 96% of the results are within 2σ of the expected values. In Table 1, for $m > 100$ µgC, the blank values are identical for CHS2-GIS and for the ampoule-cracker as their limit ages are respectively 45.9 ± 3.2 and 46.7 ± 2.9 ky BP (0.0033 ± 0.0013 and 0.0030 ± 0.0011). However, for smaller masses, we can clearly distinguish two different behaviors with a greater blank for CHS2-GIS than with the ampoule cracker introduction mode: 34.7 ± 5.4 against 41.8 ± 3.1 ky BP (0.0133 ± 0.0091 and 0.0055 ± 0.0021), which indicates higher constant contamination parameters for CHS2.

The contamination correction parameters for the CHS2-GIS were calculated from the IAEA-C1 and from the active sample ratios. These parameters are estimated at 0.31 ± 0.13 µgC with a ratio around 0.43 ± 0.06 ($F^{14}C$) and are slightly higher than the ones estimated by Fagault et al. (2019) (0.18 µgC with a $F^{14}C$ ratio of 0.14). The parameter Φ was set to the same value as for EA-GIS, at 0.004 ± 0.002 , considering that the cross contamination comes from the GIS zeolite trap. For the Ampoule cracker GIS system, carbonate sample preparation was done off-line and the contaminant was estimated from the blank IAEA-C1 to be around 0.15 ± 0.03 µgC with a ratio around 0.6 ± 0.12 $F^{14}C$. This is slightly higher than the one given by Fahrni et al. (2010) (0.1 µgC and 0.5 $F^{14}C$ ratio, uncertainties are not given). No measurable systematic cross-contamination effect was observed, and this parameter is not specified in the literature either. However, to minimize the impact of the cross contamination, samples are sorted and analyzed from the youngest to the oldest as is done for CHS2-GIS measurements.

Tube Preservation

If we compare blank values, and contamination parameters for carbonates and organic samples, it is clear that extracting the CO_2 off line and using the ampoule cracker introduction mode is the best protocol for precise small ^{14}C analysis. Another advantage of collecting and sealing the CO_2 sample in a tube is shown in Figure 4 where $F^{14}C$ values are represented, for all the IAEA-C1 blank and IAEA-C2 standards which have been sealed in tubes on the BCA line and measured via the ampoule cracker-GIS mode since 2016. The X-axis represents the time elapsed between tube sealing and tube measurement. No significant contamination with time from one day to 1 year before measurement is observed, whether for small or large samples, meaning that the CO_2 samples are perfectly well preserved in the sealed tubes.

Contamination Correction before or after Normalization

In Figure 3a, 2 different contamination corrections are depicted for Oxa2 and IAEA-C8 standards. The $F^{14}C$ ratio is corrected before steps 3, 4 and 5 (black squares) or after (blue squares). For both correction types, there was almost no difference concerning the values

(similar within the 1σ uncertainty), and uncertainties are nearly the same (they are not shown on the blue squares to make the Figure easier to read). However, small subtle differences can be systematically observed.

IAEA-C8 data corrected at the end (Figure 3a, blue squares, average of 0.1477 ± 0.0057 $F^{14}C$, all sample masses were considered, $N=38$), give slightly lower results than when corrected at step 2 (black squares, 0.1503 ± 0.0049). The difference has been averaged at 0.0026 ± 0.0014 . In fact, this gap corresponds to the blank value that is subtracted: when the contaminant correction is applied at the end, the subtracted blank value also includes the constant contaminant (even if the blank mass is high). For instance, in Table 1, (without step 2 correction) for a PHA mass $> 100 \mu gC$, the blank is at 0.0050 ± 0.0012 $F^{14}C$. When step 2 correction was applied, this blank was calculated at 0.0025 ± 0.0007 (average calculated from the black squares of Figure 3a for a PHA mass $> 100 \mu gC$). So, applying the constant contaminant correction after blank subtraction and normalization will lead to an over-correction. By applying the constant contamination correction only at step 2, the subtracted blank will be much smaller and the contaminant correction is done only once, at the beginning. The gap is not very pronounced on IAEA-C8 but could have more impact and lead to inaccuracies for ratios closer to the blank values if the contamination correction is done after normalization.

The opposite is observed for Oxa2 values. When corrected at the end (Figure 3a, blue squares, average of 1.3492 ± 0.0157 $F^{14}C$, all sample masses were considered, $N=143$), the ratios give higher values than when corrected at step 2 (black squares, 1.3417 ± 0.0147), with an average difference of -0.0075 ± 0.0036 . This can be attributed to the fact that, when normalizing the sequence with the Oxa2, the average of the chosen standard values is set at 1.3406, whether correction is done at step 2 or not. So by applying the constant contamination correction after normalization, as r_c is smaller than the Oxa2 ratio, it will mathematically increase the final standard values, and lead again to small inaccuracies.

At LSCE, we decided to apply the contamination and blank correction before normalization because it is more meaningful to normalize a sequence with a “decontaminated” standard ratio (i.e. independent of mass) and it is more accurate, especially for old samples (the subtracted blank is too high if it is not corrected from the contaminant).

CONCLUSION

Since 2016, over 5600 gas targets have been analysed with the GIS coupled to ECHOMICADAS. Nearly half of them are blanks, standards and chemical standards, regularly measured, in order to characterize the contamination for each CO_2 introduction mode: EA-GIS, CHS2-GIS and ampoule cracker.

In this paper, we have described the contamination model which is used to correct the data based on a constant and cross-contamination correction. We give an overview of all the data processing steps, and the corrections which are applied on $^{14}C/^{12}C$ ratios. The specificity of contamination correction at LSCE is that it is applied before the blank and normalization steps. For the EA-GIS introduction mode, IAEA-C7 (0.4951) and IAEA-C8 (0.1503) are in accordance with the expected $F^{14}C$ values with respectively 0.4950 ± 0.06 ($N = 27$) and 0.1512 ± 0.0027 ($N = 21$), (sample mass $35 < m < 100 \mu gC$), and the contaminant parameters are also similar to the ones observed in other laboratories ($m_c = 1.10 \pm 0.13 \mu gC$, $r_c = 0.60 \pm 0.12$ $F^{14}C$ and $\Phi = 0.004 \pm 0.002$). For carbonate samples, IAEA-C2 are also in accordance with

the expected $F^{14}\text{C}$ value (0.4114), whatever the CHS2-GIS or ampoule cracker introduction mode: respectively 0.4084 ± 0.0034 ($N = 8$) and 0.4081 ± 0.0047 ($N = 3$). Concerning the contamination parameters, for CHS2-GIS introduction they were estimated at $mc = 0.31 \pm 0.13 \mu\text{gC}$, $rc = 0.43 \pm 0.06$ and $\Phi = 0.004 \pm 0.002$. These values are a little higher than those reported in the literature, but are low enough to provide satisfactory blank values (44.4 ky BP for $35 < \text{mass} < 100 \mu\text{gC}$). For the ampoule-cracker, the contamination parameters are similar to those found in the literature ($mc = 0.15 \pm 0.03 \mu\text{gC}$, $rc = 0.6 \pm 0.12$). Regarding these contamination parameters, for carbonate samples, ampoule cracker introduction is preferred for smaller samples ($< 20 \mu\text{gC}$) or old samples, even if tube sealing is more time-consuming (off-line production rate: 5 tubes a day). For bigger carbonates, even if the contaminant is higher, the CHS2-GIS introduction mode is easier to run.

Dating small samples is still a challenge as we have to continuously monitor the evolution of the contamination parameters in order to obtain more accurate ratios. Knowing these parameters is helpful when taking decisions on 1) the analytical feasibility, with a possible estimation of the final uncertainty, 2) on the amount of material required for the sampling, and 3) on the chosen introduction mode.

ACKNOWLEDGMENTS

The ECHoMICADAS and surrounding equipment were funded by Ile de France Region, the BNP Paribas foundation, the ERDF program, the labex BCDiv and the laboratory's own resources. Thanks to the technical infrastructures PANOPLY and RegeF-AMS platforms for their help.

Thanks are due to all the people who spend their time preparing and weighing the samples at LSCE, GEOPS and MNHN laboratories. We would also like to thank Elisabeth Rowley-Jolivet for her English corrections.

REFERENCES

- Aerts-Bijma AT, Paul D, Dee MW, Palstra SWL, Meijer HAJ. 2021. An independent assessment of uncertainty for radiocarbon analysis with the new generation high-yield accelerator mass spectrometers. *Radiocarbon* 63:1–22.
- Bard E, Tuna T, Fagault Y, Bonvalot L, Wacker L, Fahrni S, Synal H-A. 2015. AixMICADAS, The accelerator mass spectrometer dedicated to ^{14}C recently installed in Aix-en-Provence, France. *Nuclear Instruments & Methods in Physics Research Section B-Beam Interactions with Materials and Atoms* 361:80–86.
- Fagault Y, Tuna T, Rostek F, Bard E. 2019. Radiocarbon dating small carbonate samples with the gas ion source of AixMICADAS. *Nuclear Instruments & Methods in Physics Research Section B-Beam Interactions with Materials and Atoms* 455:276–283.
- Fahrni S, Gägeler H-W, Hajdas I, Ruff M. 2010. Direct measurements of small ^{14}C samples after oxidation in quartz tubes. *Nuclear Instruments & Methods in Physics Research Section B-Beam Interactions with Materials and Atoms* 268:787–789.
- Hatté C, Arnold M, Dapoigny A, Daux V, Delibrias G, Du Boisgheue D, Fontugne M, Gauthier C, Guillier M-T, Jacob J, Jaudon M, Kaltnecker É, Labeyrie J, Noury C, Paterne M, Pierre M, Phouybanhdyt B, Poupeau J-J, Tannau J-F, Thil F, Tisnérat-Laborde N, Valladas H. 2023. Radiocarbon dating on EchoMICADAS, LSCE, Gif sur Yvette, France: new updated and chemical procedures. *Radiocarbon* [this proceedings]. doi: [10.1017/RDC.2023.46](https://doi.org/10.1017/RDC.2023.46)
- Hua Q, Zoppi U, Williams A-A, Smith A-M. 2004. Small-mass AMS radiocarbon analysis at ANTARES. *Nuclear Instruments & Methods in Physics Research Section B-Beam Interactions with Materials and Atoms* 223–224:284–292.
- Hwang J, Druffel ERM. 2005. Blank correction for $\Delta^{14}\text{C}$ measurements in organic compound classes of oceanic particulate matter. *Radiocarbon* 47: 75–87.

- Knowles TDJ, Monaghan PS, Evershed RP. 2019. Radiocarbon sample preparation procedures and the first status report from the Bristol Radiocarbon AMS (BRAMS) Facility. *Radiocarbon* 61:1541–1550.
- Ruff M, Fahrni S, Gäggeler HW, Hajdas I, Suter M, Synal H-A, Szidat S, Wacker L. 2010a. Online radiocarbon measurements of small samples using elemental analyzer and MICADAS gas ion source. *Radiocarbon* 52(4): 1645–1656.
- Ruff M, Szidat S, Gäggeler HW, Suter M, Synal H-A, Wacker L. 2010b. Gaseous radiocarbon measurements of small samples. *Nuclear Instruments and Methods in Physics Research B* 268(7–8):790–794.
- Ruff M, Wacker L, Gäggeler HW, Suter M, Synal H-A, Szidat S. 2007. A gas ion source for radiocarbon measurements at 200 kV. *Radiocarbon* 49(2):307–314.
- Salazar G, Zhang YL, Agrios K, Szidat S. 2015. Development of a method for fast and automatic radiocarbon measurement of aerosol samples by online coupling of an elemental analyzer with a MICADAS AMS. *Nuclear Instruments & Methods in Physics Research Section B-Beam Interactions with Materials and Atoms* 361: 163–167.
- Synal H-A, Stocker M, Suter M. 2007. MICADAS: A new compact radiocarbon AMS system. *Nuclear Instruments & Methods in Physics Research Section B-Beam Interactions with Materials and Atoms* 259:7–13.
- Stuiver M, Polach HA. 1977. Discussion: reporting of ^{14}C data. *Radiocarbon* 19(3):355–363.
- Sun S, Meyer VD, Dolman AM, Winterfeld M, Hefter J, Dummann W, McIntyre C, Montluçon DB, Haghypour N, Wacker L, Gentz T, Van der Voort T, Eglinton TI, Mollenhauer G. 2020. ^{14}C Blank Assessment in Small-Scale Compound-Specific Radiocarbon Analysis of Lipid Biomarkers and Lignin Phenols. *Radiocarbon* 62:207–218.
- Tisnérat-Laborde N, Poupeau J-J, Tannau J-F, Paterne M. 2001. Development of a semi-automated system for routine preparation of carbonate samples. *Radiocarbon* 43:299–304.
- Tisnérat-Laborde N, Thil F, Synal H-A, Cersoy S, Hatté C, Gauthier C, Massault M, Michelot J-L, Noret A, Siani G, Tombret O, Vigne J-D and Zazzo A. 2015. ECHoMICADAS: a new compact AMS system to measuring ^{14}C for Environment, Climate and Human Sciences, 22nd International Radiocarbon Conference, Dakar, Senegal, PHYS-O.05.
- Wacker L, Christl M, Synal H-A. 2010. Bats: a new tool for AMS data reduction. *Nuclear Instruments & Methods in Physics Research Section B-Beam Interactions with Materials and Atoms* 268(7–8): 976–979.
- Wacker L, Fahrni SM, Hajdas I, Molnar M, Synal H-A, Szidat S, Zhang YL. 2013. A versatile gas interface for routine radiocarbon analysis with a gas ion source. *Nuclear Instruments & Methods in Physics Research Section B-Beam Interactions with Materials and Atoms* 294:315–319.

APPENDIX A. UNCERTAINTY CALCULATION

The uncertainty formulas are obtained from the quadratic sum of the different partial derivatives of the formulas for each step described in the main document. For the notation, σ_{yyy} is the uncertainty associated to $R(X)_{yyy}$ where the subscripts yyy could be replaced by *mol*, *cont*, *bl*, *f* and *std* which refer respectively to the molecular correction ($^{13}\text{C}_{\text{mol}}$), the contaminant correction, the blank subtraction, the fractionation correction and the standard normalization.

Step 1: Molecular correction uncertainty

In the first calculation step, the measured $^{14}\text{C}/^{12}\text{C}$ ratio is corrected for broken up molecules ^{13}CH and this correction is proportional to the $^{13}\text{C}_{\text{mol}}$ current. Whereas the uncertainty of the $^{14}\text{C}/^{12}\text{C}$ ratio is directly linked to the ^{14}C counting statistic (Poisson statistical law), at LSCE, for the ECHoMICADAS instrument, the uncertainty of the factor k_{mol} (noted $\sigma_{k_{\text{mol}}}$) is set at 30% of this value ($k_{\text{mol}} = 150 \pm 50$).

$$\sigma_{\text{mol}} = \frac{\sqrt{{}^{14}\text{C} + (\sigma_{k_{\text{mol}}} * {}^{13}\text{C}_{\text{mol}})^2}}{^{12}\text{C}}$$

Step 2: Uncertainty calculation linked to constant contamination (σ_{m_c} and σ_{r_c}) and to cross contamination (σ_Φ) uncertainty propagations.

$$\sigma_{mol,cont} = \left\{ \left(\frac{m_0 * (m_1 * (R(X)_{mol} - R(X_0)_{mol}) + m_c * (R(X_0)_{mol} - r_c))}{(m_1 - m_c - \Phi * m_0)^2} * \sigma_\Phi \right)^2 + \left(\frac{m_c}{m_1 - m_c - \Phi * m_0} * \sigma_{r_c} \right)^2 + \left(\frac{m_1 * (R(X)_{mol} - R_c) + \Phi * m_0 * (r_c - R(X_0)_{mol})}{(m_1 - m_c - \Phi * m_0)^2} * \sigma_{m_c} \right)^2 + \left(\frac{m_1}{m_1 - m_c - \Phi * m_0} * \sigma_{mol} \right)^2 \right\}^{1/2}$$

Step 3: Uncertainty calculation linked to the blank correction

Historically, at LSCE, to calculate the blank uncertainty, we take the maximum between the weighted standard deviation of the selected blanks measured during the sequence and σ_{bl} , the uncertainty which can take into account the blank variability on a longer period: at LSCE this value is generally taken as 30%. For blank F¹⁴C values, the blank is not subtracted, so σ_{bl} is set to 0.

$$\sigma_{\langle R(bl)_{mol,cont} \rangle} = \max \left\{ \sigma_{bl} * \langle R(bl)_{mol,cont} \rangle, \left\{ \frac{1}{\sum_i p_i} * \sum_i (p_i * (R(bl_i)_{mol,cont} - \langle R(bl)_{mol,cont} \rangle)^2) \right\}^{1/2} \right\}$$

It allows to calculate:

$$\sigma_{mol,cont,bl} = \left\{ \sigma_{mol,cont}^2 + \sigma_{\langle R(bl)_{mol,cont} \rangle}^2 \right\}^{1/2}$$

Step 4: Uncertainty linked to the fractionation correction

$$\sigma_{\delta^{13}C(X)} = (1 + \delta^{13}C(X)) * \left\{ \left(\frac{\sigma_{R_{13}(X)}}{R_{13}(X)} \right)^2 + \left(\frac{\sigma_{\delta^{13}C_{Std}}}{1 + \delta^{13}C_{Std}} \right)^2 + \left(\frac{\sigma_{\langle R_{13}(Std) \rangle}}{\langle R_{13}(Std) \rangle} \right)^2 \right\}^{1/2}$$

$\sigma_{R_{13}(X)}$ is calculated from the current measurement precision (estimated at $\sigma_nC = 0.0001 * nC$, with n = 12 or 13):

$$\sigma_{R_{13}(X)} = R_{13}(X) * \left\{ \left(\frac{\sigma_{12C}}{12C(X)} \right)^2 + \left(\frac{\sigma_{13C}}{13C(X)} \right)^2 \right\}^{1/2} = 0.0001 * R_{13}(X) * \sqrt{2}$$

$\sigma_{\delta^{13}C_{Std}}$ is the uncertainty of the $\delta^{13}C$ standard value (here 0.0001, for the Oxa2 standard which is -17.8 ± 0.1 ‰)

$\sigma_{\langle R_{13}(Std) \rangle}$ is the uncertainty linked to the standard reproducibility in the sequence. It is estimated with the weighted standard deviation of the ratio.

$$\sigma_{\langle R_{13}(Std) \rangle} = \left\{ \frac{1}{\sum_i p_i} * \sum_i (p_i * (R_{13}(std_i) - \langle R_{13}(Std) \rangle)^2) \right\}^{\frac{1}{2}}$$

$\sigma_{R_{13}(X)}$ and $\sigma_{\delta^{13}C_{Std}}$ values which are around 0.1‰ are negligible compared to $\sigma_{\langle R_{13}(Std) \rangle}$ which can sometimes reach several ‰ units. For example, the standard deviation of the $\delta^{13}C$ values for the oxa2 presented in this manuscript for sample masses > 50 µgC is around 2.5‰ (N=62).

From this calculated $\sigma_{\delta^{13}C(X)}$, and the previous equations we can calculate

$$\sigma_{mol,cont,bl,f} = R(X)_{mol,cont,bl,f} * \left\{ \left(\frac{\sigma_{mol,cont,bl}}{R(X)_{mol,cont,bl}} \right)^2 + \left(\frac{2 * \sigma_{\delta^{13}C(X)}}{1 + \delta^{13}C(X)} \right)^2 \right\}^{\frac{1}{2}}$$

For small samples $\sigma_{\delta^{13}C(X)}$ is rapidly negligible compared to $\frac{\sigma_{mol,cont,bl}}{R(X)_{mol,cont,bl}}$

Step 5: Normalization step: as in step 3, we have first to calculate the standard deviation of Oxa2 ratios. We keep the possibility of adding a σ_{ex} corresponding to an additional uncertainty linked to the real standard deviation of the standard oxa2 with longer time period and not only during one sequence. At LSCE, this value is set at 0.005 for GIS samples.

$$\sigma_{\langle R(std)_{mol,cont,bl,f} \rangle} = \max \left\{ \begin{array}{l} \sigma_{ex} * \langle R(std)_{mol,cont,bl,f} \rangle, \\ \left\{ \frac{1}{\sum_i p_i} * \sum_i (p_i * (R(Std_i)_{mol,cont,bl,f} - \langle R(std)_{mol,cont,bl,f} \rangle)^2) \right\}^{\frac{1}{2}} \end{array} \right\}$$

From this, the final formula with $\sigma_{R_{nom}}$, the uncertainty of the official standard $F^{14}C$ ratio R_{nom} can be calculated:

$$\sigma_{mol,cont,bl,f, std} = R(X)_{mol,cont,bl,f, std} * \left\{ \left(\frac{\sigma_{R_{nom}}}{R_{nom}} \right)^2 + \left(\frac{\sigma_{mol,cont,bl,f}}{R(X)_{mol,cont,bl,f}} \right)^2 + \left(\frac{\sigma_{\langle R(std)_{mol,cont,bl,f} \rangle}}{\langle R(std)_{mol,cont,bl,f} \rangle} \right)^2 \right\}^{\frac{1}{2}}$$